Marine and Petroleum Geology 98 (2018) 640–652

Contents lists available at ScienceDirect

Marine and Petroleum Geology

journal homepage: www.elsevier.com/locate/marpetgeo

Research paper

# Vertical effective stress as a control on quartz cementation in sandstones

Olakunle J. Oye[a,**], Andrew C. Aplin[a,*], Stuart J. Jones[a], Jon G. Gluyas[a], Leon Bowen[b], Ian J. Orland[c], John W. Valley[c]

[a] Department of Earth Sciences, Durham University, Durham, DH1 3LE, UK
[b] Department of Physics, Durham University, Durham, DH1 3LE, UK
[c] WiscSIMS Lab, Department of Geoscience, University of Wisconsin, Madison, WI, 53706-1692, USA

ARTICLE INFO

*Keywords:*
Sandstone
Diagenesis
Quartz cement
Effective stress
Secondary ion mass spectrometry
Oxygen isotopes

ABSTRACT

Temperature-controlled precipitation kinetics has become the overwhelmingly dominant hypothesis for the control of quartz cementation in sandstones. Here, we integrate quantitative petrographic data, high spatial resolution oxygen isotope analyses of quartz cement, basin modelling and a kinetic model for quartz precipitation to suggest that the supply of silica from stress-sensitive intergranular pressure dissolution at grain contacts is in fact a key control on quartz cementation in sandstones. We present data from highly overpressured sandstones in which, despite the current burial temperature of 190 °C, quartz cement occurs in low amounts (4.6 ± 1.2% of bulk volume). In situ oxygen isotope data across quartz overgrowths suggest that cementation occurred over 100 Ma and a temperature range of 80–150 °C, during which time high fluid overpressures resulted in consistently low vertical effective stress. We argue that the very low amounts of quartz cement can only be explained by the low vertical effective stress which occurred throughout the burial history and which restricted silica supply as a result of a low rate of intergranular pressure dissolution at grain contacts.

## 1. Introduction

During basin subsidence, the precipitation of macroquartz cement is a key process by which sands become sandstones. Resultant changes in physical properties exert a primary control on the ability of sandstones to store and to transmit fluids: on a basin-scale as a control on the transfer of fluid pressure (Reilly and Flemings, 2010; Yardley and Swarbrick, 2000), and on a more local scale in the context of $CO_2$ storage, the development of low enthalpy geothermal energy resources and petroleum production. Given its importance as a geological process, many studies have examined the potentially multifaceted controls of macroquartz cementation and the underlying processes of supply, transport and precipitation of silica (e.g. Bloch et al., 2002; Taylor et al., 2010; Worden and Morad, 2000). Currently, the dominant hypothesis is that the rate-limiting step in macroquartz cementation is precipitation, such that the rate of macroquartz cementation is geologically negligible below 80 °C but then increases exponentially with temperature (Ajdukiewicz and Lander, 2010; Walderhaug, 1994a, 1996). In addition, early-formed grain coatings of microquartz and clay have been shown to inhibit the precipitation of macroquartz cement (Aase et al., 1996; Ajdukiewicz et al., 2010; Bloch et al., 2002; Heald and Larese, 1974; Osborne and Swarbrick, 1999; Stricker et al., 2016a; Worden and Morad, 2000), and there is continuing debate about the extent to which petroleum acts as a brake on cementation by altering the wetting state of grains and/or increasing the tortuosity of diffusion pathways (Marchand et al., 2002; Sathar et al., 2012; Worden and Morad, 2000; Worden et al., 1998, 2018b). Predictive, computer-based models of macroquartz cementation incorporate these ideas and have become the dominant concepts for modelling both macroquartz cementation and the related loss of porosity and permeability (Ajdukiewicz and Lander, 2010; Lander and Walderhaug, 1999; Walderhaug, 1996).

Silica supply is not deemed to be important in current cementation models (Lander and Walderhaug, 1999; Walderhaug, 1996, 2000). Intergranular pressure dissolution and the linked process of stylotization are seen as key sources of silica but have fallen out of favour as a rate-controlling process. Intergranular pressure dissolution, or chemical compaction, occurs at grain contacts because the chemical potential of silica at stressed, grain-grain contacts is enhanced over that in the bulk solution (De Boer et al., 1977; Dewers and Ortoleva, 1990; Elias and Hajash, 1992; Gratier et al., 2005; Renard et al., 1997; Sheldon et al., 2003; Shimizu, 1995; Tada and Siever, 1989; van Noort et al., 2008).

* Corresponding author.
** Corresponding author.
*E-mail addresses:* o.j.oye@durham.ac.uk (O.J. Oye), a.c.aplin@durham.ac.uk (A.C. Aplin).

https://doi.org/10.1016/j.marpetgeo.2018.09.017
Received 13 May 2018; Received in revised form 13 September 2018; Accepted 14 September 2018
Available online 17 September 2018

Silica is thus released at stressed interfaces and precipitates on free quartz faces. Since the enhancement of chemical potential is a function of effective stress (Elias and Hajash, 1992; Sheldon et al., 2003), it is rational that the rate of intergranular pressure dissolution and thus of silica supply would be related to vertical effective stress (VES), and thus the history of VES through time. However, whilst some studies (Elias and Hajash, 1992; Osborne and Swarbrick, 1999; Sheldon et al., 2003; van Noort et al., 2008) support the idea that intergranular pressure dissolution in sandstones is related to maximum effective stress, others (Bjørkum et al., 1998; Oelkers et al., 1996; Walderhaug, 1996) suggest that the process is "stress-insensitive" and catalysed by sheet silicates (clays and micas), with the rate being controlled mainly by temperature (Lander and Walderhaug, 1999; Walderhaug, 2000).

In order to test the role of vertical effective stress on macroquartz cementation, we report here the results of a study in which sandstones currently buried to 190 °C contain much lower amounts of macroquartz cement than is predicted by temperature-related macroquartz cementation models. Fluids within the sandstones are highly overpressured and the current vertical effective stress is low, suggesting that vertical effective stress may have limited macroquartz cementation due to a restriction in the rate of silica supply via intergranular pressure dissolution. However, other factors such as microquartz and clay coatings are known to influence quartz cementation and must be evaluated, and it is the *history* of vertical effective stress rather than the current vertical effective stress which would be expected to control the extent of silica supply via intergranular pressure dissolution.

Here, therefore, we integrate (a) detailed, quantitative petrographic analyses of cements and grain coatings, (b) high spatial resolution oxygen isotope analyses of macroquartz cement, (c) basin modelling, and (d) kinetic modelling of quartz precipitation in order to evaluate the hypothesis that it is the history of vertical effective stress, rather than that of temperature, that is a key control on macroquartz cementation.

## 2. Geological setting

Elgin is part of the high pressure, high temperature (HPHT) area of the Central North Sea located in United Kingdom Quadrant 22, blocks 22, 24, 29 and 30, about 240 km east of Aberdeen. It is surrounded by other producing fields including: Shearwater to the north east, Glenelg to the west, and Franklin to the south (Fig. 1). The Elgin area experienced extensional events in the Triassic and the Late Jurassic/Early Cretaceous prior to minor compression phases that span the Neogene (Eggink et al., 1996; Lasocki et al., 1999). Structurally, the field is an anticline bounded by sub-vertical faults, and also traversed and compartmentalised by sealing NW-SE trending minor normal faults (Lasocki et al., 1999). The general structure of the field has been significantly influenced by halokinesis. Elgin field is a complex, structural anticlinal trap (Lasocki et al., 1999) with the Upper Jurassic shallow marine Fulmar sandstone as the main reservoir and an average thickness of about 300 m. The reservoir contains gas condensate charged mainly from two sources: Upper Jurassic Kimmeridge Clay and Heather Formations (Isaksen, 2004; Lasocki et al., 1999). The Paleogene and Neogene in the Elgin area were marked by accumulation of thick deposits of the Nordland and Hordaland shales. The rapid deposition of these Formations, together with the low permeability Cretaceous Chalk group, restricted fluid flow, thus initiating and maintaining high formation pressures in the reservoir sandstones (Darby et al., 1996). The present-day fluid pressure and temperature in the Upper Jurassic Fulmar sandstone in the Elgin field are around 110 MPa and 190 °C (Lasocki et al., 1999). At these conditions, the Fulmar sandstone reservoir in the Elgin area is one of the deepest, hottest and most highly overpressured in the Central North Sea.

## 3. Fulmar formation sedimentology and stratigraphy

The Upper Jurassic Fulmar Formation is the primary hydrocarbon producing reservoir in many oil fields in the UK sector of the Central Graben. Apart from the northwest of the Elgin field where the Base Cretaceous Unconformity (BCU) erodes down to the Fulmar level, the Formation (Fig. 2) is overlain conformably by the Heather and the Kimmeridge Clay Formations (Lasocki et al., 1999). The Pentland Formation underlying the Fulmar is also perceived to be virtually conformable in the axial part of the Central Graben (Lasocki et al., 1999). The Upper Jurassic Fulmar Formation is a highly bioturbated, heterolithic, shallow-marine sand-silt deposit (Gowland, 1996), and often occurs as a coarsening-upward succession grading from siltstones into very fine-medium-grained sandstone (Gowland, 1996; Hendry et al., 2000; Lasocki et al., 1999; Stewart, 1986; Taylor et al., 2015). Occasional fining-upward successions have also been delineated locally (Gowland, 1996; Lasocki et al., 1999). The dearth of sedimentary structures due to intense bioturbation, and the influence of synsedimentary tectonism and halokinesis created complicated facies patterns within the Fulmar sandstone (Gowland, 1996; Hendry et al., 2000). Hence, facies characterisation of these sandstones often requires a more detailed study of lithology, grain size, sedimentary structures (where present) and ichnofabrics like *Teichicnus* and *Ophiomorpha* (Gowland, 1996; Taylor and Gawthorpe, 1993). Depositional profile delineation using lithofacies and ichnofabric descriptions show that upper shoreface to offshore transition zones predominate in the Fulmar Formation of the Elgin field (Lasocki et al., 1999). The occurrence of abundant rock-forming siliceous sponge spicules, of the genus *Rhaxella*, have been reported in some intervals within the Fulmar Formation (Gowland, 1996). Gowland (1996) and Taylor et al. (2015) described these *Rhaxella* sponge spicules as the likely source of grain-coating microcrystalline quartz in the Fulmar sandstone. Helium porosities of up to 30% in some deeply buried clean facies indicate that these sandstones are anomalously porous relative to other North Sea sandstones (Osborne and Swarbrick, 1999).

## 4. Methodology

### 4.1. Sampling strategy

Core samples investigated in this study were selected from the Upper Jurassic Fulmar Formation in Elgin field (22/30C-G4), where the present-day vertical effective stress and temperature of 12.5 MPa and 189 °C respectively. The Fulmar sandstones in the Elgin field are most probably at their maximum burial depth, pore pressure and temperature conditions. In order to limit the number of depositionally-related variables which are considered to influence quartz cementation, sampling focussed on a single Fulmar sandstone facies based on the characteristics described by Gowland (1996). Hence, nineteen samples were selected from clean, upper shoreface sandstone facies, mainly the "B" sands (Fig. 2), between 5400 and 5440 m true vertical depth sub-sea (TVDSS).

### 4.2. Petrography

Petrographic analyses were carried out on rock chips and thin sections prepared from core samples using optical microscopy, and combined scanning electron microscope and cathodoluminescence (SEM-CL) microscopy. The standard petrographic work was conducted using a Leica DM 2500P microscope fitted with a light-emitting diode (LED) illumination source. A Conwy Valley Systems Limited Petrog digital petrography system was integrated with the Leica microscope for quantification work. This allows a systematic calculation of the proportion of grain types, grain contacts, grain coats, matrix and cement by making not less than 300 point counts per thin section (Nichols, 2009).

Optical microscopy revealed that carbonate cements are

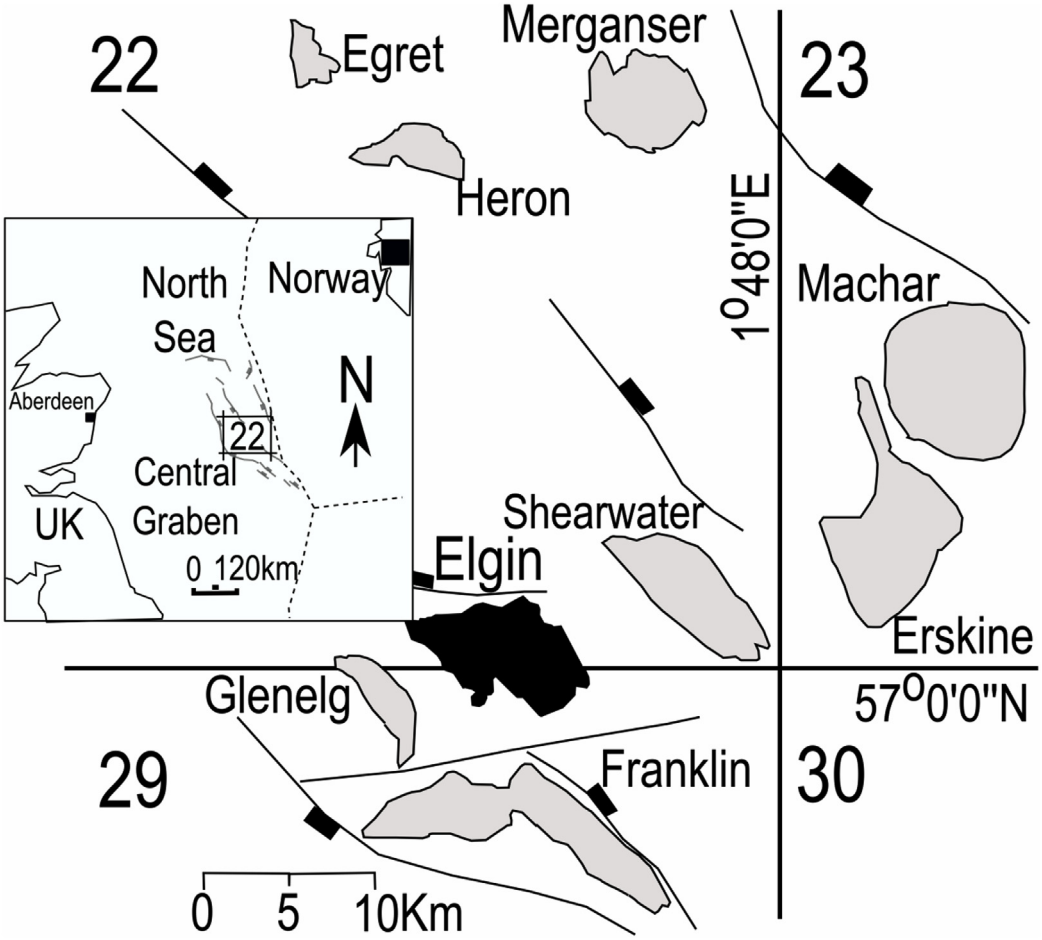


**Fig. 1.** Map of the Central Graben in the UK North Sea showing Elgin field and other surrounding hydrocarbon fields.

heterogeneously distributed in the sample sets. Since early carbonate cement can significantly occlude porosity and thus bias quartz cement results, these samples were rejected from the sample set. Overall, ten carbonate-free samples representing the full range of quartz cement contents were analysed using cathodoluminescence (CL) petrography.

Whilst based on well-established concepts (Evans et al., 1994; Houseknecht, 1991; Sibley and Blatt, 1976), we developed an improved SEM methodology with which to quantify the amounts of overlap and authigenic quartz over statistically meaningful sample areas. CL imaging used a Gatan mono-CL3 detector connected to a Hitachi SU-70 Analytical UHR Schottky Emission Scanning Electron Microscope. An Oxford Instruments energy dispersive x-ray (EDX) system (X-MaxN 50 Silicon Drift Detector) was used to obtain the Si element map. Panchromatic CL images were obtained at ×300 magnification, 1024 × 1024 resolution, from predefined 3 mm × 3 mm areas from each thin section. A mosaic of about 70 frames of CL images, representing the 9 $mm^2$ area, was acquired in 1 h. The CL mirror was then retracted to allow Si maps to be acquired over the same area, so that a complete CL and EDX data set was acquired in 7 h. Using the Si element map to identify quartz and the CL to identify quartz cement (Fig. S2), we then manually point-counted both overlap quartz (points of quartz to quartz grain dissolution) and authigenic quartz using a grid of 1600 (40 × 40) square boxes superimposed on the CL image. The central point in each box is counted, generating 1600 data points per sample.

### 4.3. Effective stress and temperature histories

The evolution of sedimentary basins and hydrocarbon reservoirs through time can be reconstructed using basin modelling software. A one-dimensional basin modelling approach was adopted to evaluate the evolution of temperature and effective stress in the Fulmar Formation reservoir. Although the technique is limited by its inability to model lateral fluid flow and hydrocarbon charge, overpressure generation from compaction disequilibrium can be effectively simulated. Compaction disequilibrium is generally the most quantitatively important overpressure generation mechanism; other processes, such as gas generation, may have also contributed to overpressure, and would act to reduce the effective stress through time. The one-dimensional modelling work was carried out using Schlumberger's PetroMod software (Version 2014.1). The software uses a forward modelling approach to reconstruct the burial histories of sedimentary basins. The present-day stratigraphic layers and thicknesses, lithology and lithological description used for the modelling were obtained from well composite logs, geological well reports, core analysis, and core description reports (Table 1). Geological ages derived from the Millenium Atlas (Gluyas and Hichens, 2003) were used to set the model. Heat flow models were built after Allen and Allen (2005), with an average of 62 $mW/m^2$ throughout the basin's history. Heat flow values of 70 and 90 $mW/m^2$ were used to model the peaks of the Permo-Triassic and Upper Jurassic paleo-rifting events. The thermal model was calibrated using corrected bottom-hole temperatures obtained from the operator's report, plus vitrinite reflectance data. In order to model compaction, Fulmar Formation porosities from routine core analysis were incorporated in the model. Since porosity is a function of lithology, tighter constraints were placed on the model by modifying PetroMod's default lithologies to match those observed on the field. These lithologies were defined using well composite logs and core analysis descriptions. Based on this study, the Chalk Group and the Pre-Cretaceous

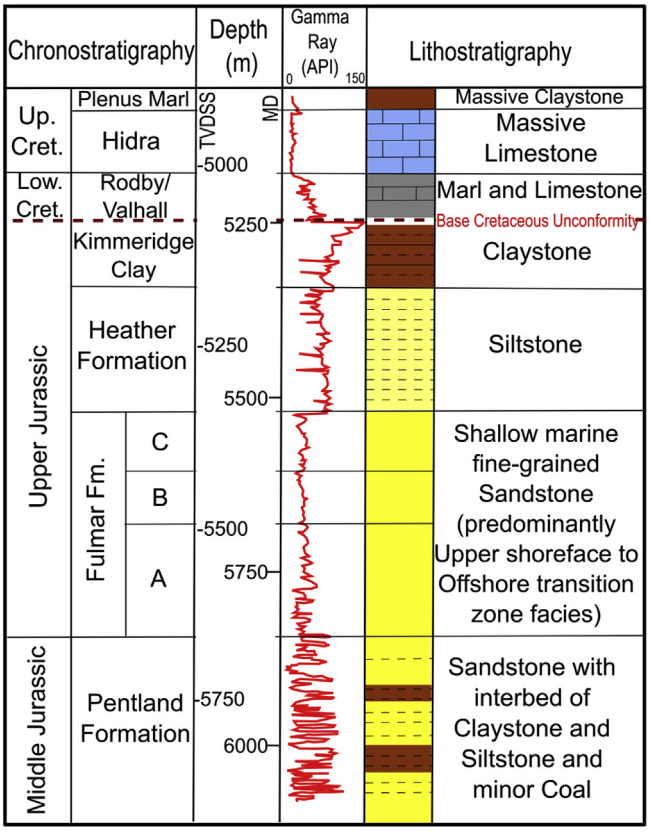


**Fig. 2.** Stratigraphy of the Middle Jurassic to Upper Cretaceous in well 22/30C-G4 of the HPHT Elgin Field, Central North Sea, UK.

shales (Kimmeridge Clay and Heather Formations) are very important for modelling the observed high pore pressure in the Fulmar Formation. The default chalk and shale permeabilities in PetroMod were modified after Swarbrick et al. (2000), to lower values for the Chalk Group and the Pre-Cretaceous shales until modelled pore pressure matched Present-day pressures.

### 4.4. Quartz precipitation kinetic modelling

Walderhaug's (1996) approach was used to model the growth of quartz cement. This mathematically simple model uses a logarithmic function of temperature to calculate the rate of quartz cementation (Walderhaug, 1996, 2000). Although there are other, more sophisticated, Arrhenius-based models in which the rate of cementation can be adjusted by changing the activation energy for quartz precipitation, these were not available for this study. However, we argue that the simpler logarithmic model generates a useful framework for any discussion of quartz cementation, partly because it was calibrated on extensive field observations from the North Sea and also because it was shown to give very similar results to those from an Arrhenius-based function in a set of sandstones from the North Sea Brent Group (Walderhaug, 2000).

The Fulmar Formation sandstones from Elgin field are arkosic - subarkosic in composition; hence, the quartz cementation model was applied to only the quartz fraction of the bulk rock. The kinetic model was run using Walderhaug's (1996) standard parameters on 1 $cm^3$ of sandstone, with a 80 °C threshold temperature for quartz cementation and a starting porosity of 26 vol % at the onset of quartz cementation. A value of $1.98 \times 10^{-22}$ $mol/cm^2s$ was used for the pre-exponential $a$, and 0.022 °C for the exponential constant $b$, calculated by Walderhaug (1994b) for some North Sea sandstones. Detrital quartz fractions and grain sizes were estimated from CL petrographic analysis of thin sections. The percentage of detrital quartz surface area with grain coats was calculated through visual inspection and manual quantification using CL, BSE and silica maps acquired over the same sample area. This method was adopted because BSE images allow easy identification of both grain-coating clays and microquartz in thin sections. Microquartz was, however, very rarely observed. The CL images also revealed where grain coatings are actually present on detrital or authigenic quartz. In order to incorporate grain-coat data into the model, the initial quartz surface area was reduced using the estimated grain coatings coverage area. This approach is similar to the method used by Walderhaug (2000). Heating rates were calculated from time-temperature histories generated from a basin model constructed using PetroMod (version 2014.1).

### 4.5. Oxygen isotope analysis

Secondary Ion Mass Spectrometry (SIMS) analysis was performed at the WiscSIMS Laboratory at the University of Wisconsin-Madison. Three separate quartz grains with overgrowths thicknesses between 40 and 60 µm were chosen for *in situ* oxygen isotope analysis. Profiles of oxygen isotope ratios were measured using a 3 µm spot diameter on a

**Table 1**
Formation thicknesses and lithotypes used for Elgin burial history modelling. Percentage values show mix ratio for interbedded Formations.

| System | Series | Group | Age (Ma) | Formation | Lithology | Thickness (m) |
|---|---|---|---|---|---|---|
| Neogene | Miocene -Pleistocene | Nordland Group (Undiff.) | 13 | Nordland Group (Undiff.) | Shale | 1416 |
| Paleogene | Eocene - Miocene | Hordaland Group (undiff.) | 54 | Hordaland Group (undiff.) | Shale | 1579 |
| Paleogene | Eocene | Rogaland | 54.3 | Balder Fm | Silty Shale 95% tuff 5% | 30 |
| Paleogene | Paleocene | Rogaland | 56 | Sele Fm | Shale 65% Sandstone 35% | 48 |
| Paleogene | Paleocene | Montrose | 57.8 | Lista Fm | Shale | 79 |
| Paleogene | Paleocene | Montrose | 58.3 | Lista Fm (Andrew Member) | Shale 65% Limestone 35% | 63 |
| Paleogene | Paleocene | Montrose | 62.5 | Maureen Fm | Shaly Limestone 90% Marl 10% | 130 |
| Paleogene | Paleocene | Chalk | 65 | Ekofisk Fm | Chalk 85% Silt 5% Clay 5% Marl 5% | 102 |
| Cretaceous | Upper | Chalk | 72 | Tor Fm | Chalk | 502 |
| Cretaceous | Upper | Chalk | 91 | Hod Fm | Chalk 90% Marl 10% | 718 |
| Cretaceous | Upper | Chalk | 93 | Herring Fm | Chalk | 144 |
| Cretaceous | Upper | Chalk | 94 | Plenus Marl Fm | Shale | 2 |
| Cretaceous | Upper | Chalk | 99 | Hidra Fm | Chalk | 85 |
| Cretaceous | Lower | Cromer Knoll | 107 | Rodby Fm | Shale 65% Limestone 30% Marl 5% | 15 |
| Cretaceous | Lower | Cromer Knoll | 128.5 | Valhall | Shale 60% Marl 40% | 49 |
| Jurassic | Upper | Humber | 153 | Kimmeridge C. Fm. | Shale (black) | 103 |
| Jurassic | Upper | Humber | 156 | Heather Fm | Shale (organic rich, typical) | 334 |
| Jurassic | Upper | Humber | 158.4 | Fulmar Sands | Sandstone (arkose, quartz rich) | 160 |
| Jurassic | Middle | Fladen | 166 | Pentland Sand | Sandstone (clay rich) | 164 |
| Jurassic | Middle | Fladen | 170 | Pentland Shale | Shale (organic rich, typical) | 110 |

CAMECA IMS 1280 ion microprobe (Kita et al., 2009). In order to correct measured $\delta^{18}O$ values to the Vienna standard mean ocean water (VSMOW) scale, bracketing standards were used to calculate the instrumental bias (Kita et al., 2009). Based on repeat analyses of the University of Wisconsin (UWQ-1, Kelly et al. (2007)) quartz standards embedded within samples cast in epoxy mount, the spot-to-spot external precision of all bracketing standards averaged 0.68‰ (2 SD) for the 3-μm spots. A more detailed SIMS analytical procedure is described in Page et al. (2007), Kita et al. (2009), Valley and Kita (2009) and Pollington et al. (2011). All data are reported in the supplementary material.

## 5. Results

### 5.1. Burial, thermal and VES histories

The burial history of the Fulmar sands is characterised by (a) 1 km of rapid burial in the late Jurassic, (b) a period of very limited deposition in the early Cretaceous and (c) rapid burial from *ca.* 100 Ma to the present-day, with particularly rapid sedimentation in the last 12 Ma. The resulting temperature, pore pressure and effective stress histories are shown in Fig. 3. With overpressure being generated from around 90 Ma, these constraints suggest that the vertical effective stress has been low throughout the entire burial history and has never been greater than the present-day value of 12.5 MPa. In terms of temperature, the Fulmar has resided within the classic > 70–80 °C quartz cementation window (Walderhaug, 1994a) for the last 90 Ma.

### 5.2. Petrographic observations

Fulmar sandstones in this study are from the clean, upper shoreface facies. They are arkosic to sub-arkosic in composition, with sub-angular to sub-rounded grain shapes. Depositional grain sizes measured from CL petrographic data range from 0.063 to 0.36 mm, with an average of 0.156 mm (Fig. S3). Clay contents (mainly illite) content are low, about 2.8% of bulk volume, reflecting our targeting of clean, upper shoreface sands. Clays are commonly bitumen-impregnated and are typically either pore-filling or forming discontinuous coats on both detrital and authigenic quartz surfaces. Complete or partial dissolution of K-feldspars and their overgrowths are common features. Where the feldspars are wholly dissolved, a moldic clay outline often preserves the original shapes (Fig. 4). Pore-filling, authigenic illite is commonly found adjacent to these dissolved feldspars, suggesting their formation from the dissolution process. Other minor components observed are micas, pyrite and bitumen. Average optical and helium porosities are 14.3 and 22% (Table 2). All petrographic data are reported in Tables S1, S2, and S3.

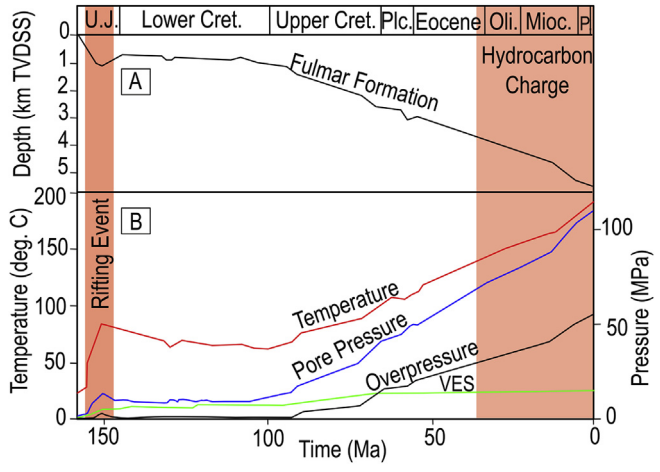


**Fig. 3.** A) Modelled burial plot with depth in meters TVDSS (true vertical depth subsea). B) Modelled temperature, pore pressure, overpressure, and vertical effective stress (VES) histories for the Upper Jurassic Fulmar Formation of the HPHT Elgin field. These models were constructed by using a forward modelling approach on PetroMod 1D version 2014.1. Overpressure was assumed to be due mainly to compaction disequilibrium, and builds from *ca.* 90 Ma. Hydrocarbons were charged to the reservoir from *ca.* 40 Ma.

Carbonate and quartz make up the main diagenetic cements. The carbonate cements average ~9% of bulk rock volume. Point count data from standard petrography and core examination shows these carbonate cements are unevenly distributed. A more detailed study on these cements was carried out by Hendry et al. (2000). Apart from dolomite and ferroan dolomites, syntaxial ankerite rims on dolomite nuclei were commonly observed in these samples. Generally, these carbonate cements either occur in isolation within available pore spaces or as pore-occluding cement, completely destroying porosity across large areas. Evidence from fluid-inclusion analysis suggests the ankerite cements were precipitated at high temperatures (140–170 °C), and their formation immediately precedes hydrocarbon emplacement in the Elgin field (Hendry et al., 2000). Although carbonate is a locally important cement, note that for the detailed quartz cementation work reported in this study, carbonate-bearing samples were rejected from the sample set.

### 5.3. Quartz cementation and chemical compaction

Two types of diagenetic quartz cements, macroquartz and microquartz, were identified as overgrowths on free detrital quartz surfaces (Figs. 4–6). In this study, the term “microquartz overgrowth” is used to describe randomly oriented, thin, polycrystalline quartz overgrowths ranging from 1 to 10 μm in length (Aase et al., 1996; French and Worden, 2013). Microquartz overgrowths were rarely observed in the analysed sandstones, with lengths around 1 μm where present (Fig. 5B). In contrast, the macroquartz overgrowths are syntaxial and blocky, and in optical continuity with detrital quartz when viewed under transmitted light. Macroquartz overgrowths are not continuous along grain boundaries and do not grow fully across available pore spaces (Fig. 4B). An important observation is that quartz overgrowths engulf some of the early-formed, grain-coating illite(Fig. 6A).

Chemical compaction is a process of rock volume reduction by stress-sensitive pressure dissolution along grains or stylolitic contacts. The released materials (e.g. silica) are then re-precipitated locally on free detrital grain surfaces. The chemical compaction estimation method used by Sibley and Blatt (1976) and Houseknecht (1991) was used to quantify the effect of intergranular pressure dissolution in the analysed sandstone samples. This quantification was performed on the same large area CL maps used to quantify quartz cement. Grain boundaries were projected along grain contacts where it appears that dissolution has taken place (Fig. 4B), and the inferred features were point-counted as percentage volumes of silica dissolved by intergranular pressure dissolution. Even though this approach is subjective, it is still the only available method for quantifying intergranular pressure dissolution in sandstone. Chemical compaction estimates from CL petrography (Fig. 4B and Table 2) suggest an average of 2.7 ± 0.8 vol % of silica was released into the system by intergranular pressure dissolution. The textural maturity of the Fulmar sandstone was factored into the quantification process to reduce uncertainties.

### 5.4. Isotopic composition of quartz cements

Similar to Harwood et al. (2013), we used high-spatial resolution SIMS to create 3-μm spot-size $\delta^{18}O$ profiles across three, 40–60 μm thick macroquartz overgrowths in one of the sandstone samples. Forty $\delta^{18}O$ measurements were made on three different quartz grains, five from detrital quartz and thirty-five from their corresponding overgrowths. Four out of the thirty-five overgrowth measurements were compromised by the occurrence of fluid inclusions or included detrital quartz, and discarded (Figs. S4 and S5, Tables S4 and S5). The remaining

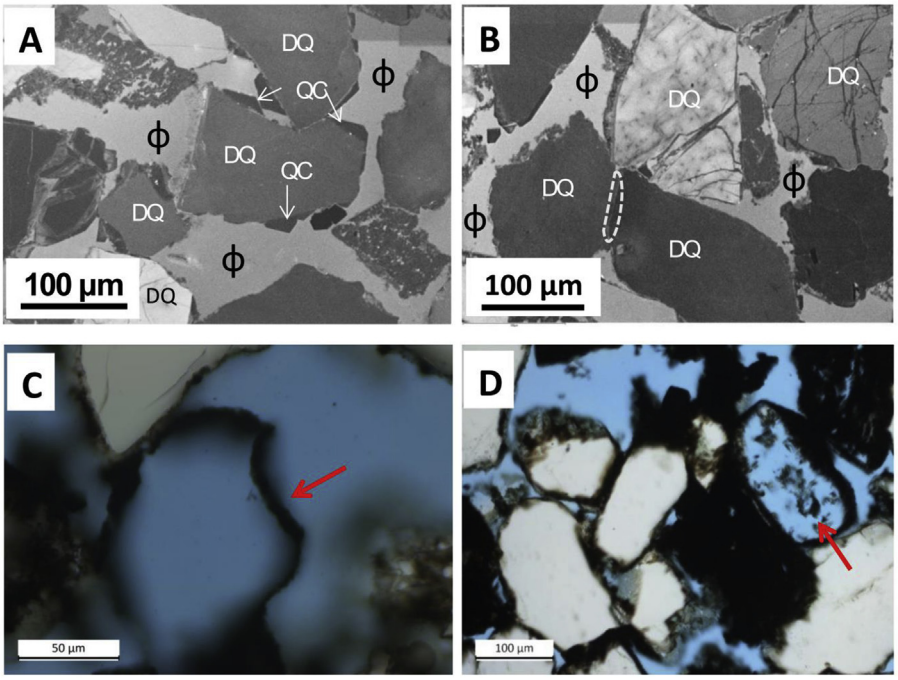


**Fig. 4.** Photomicrographs of Fulmar Formation sandstones from HPHT Elgin field in the Central North Sea; A) CL image showing quartz cement (QC) on detrital quartz (DQ). Quartz cements are poorly developed despite significant porosity and very high present-day temperature (190 °C). B) CL image showing definition of overlap quartz (pressure dissolution) in dashed trace. Red arrows in plates C and D indicate intragranular porosity due to feldspar dissolution. Original grain shape is preserved as bitumen-impregnated clay rim. (For interpretation of the references to colour in this figure legend, the reader is referred to the Web version of this article.)

**Table 2**
Petrographic analyses of the Upper Jurassic Fulmar Formation samples form Elgin Field, UK Central North Sea. More detailed data are reported in the supplementary material (Fig. S3, Tables S1, S2 and S3).

| | Mean | Standard Deviation | Minimum | Maximum | Population |
|---|---|---|---|---|---|
| Detrital grain size (mm) | 0.16 | 0.05 | 0.06 | 0.36 | 10 |
| Quartz (%) | 44.2 | 5.6 | 32.3 | 55.7 | 19 |
| Feldspar (%) | 23.5 | 3.4 | 17.3 | 29.7 | 19 |
| Lithic Fragments (%) | 1.1 | 0.7 | 0 | 2.7 | 19 |
| Quartz cement - standard petrography (%) | 2 | 1.4 | 0.3 | 6.3 | 19 |
| Quartz cement - CL petrography (%) | 4.6 | 1.2 | 2.1 | 6.4 | 10 |
| Intergranular Pressure Dissolution - CL petrography (%) | 2.7 | 0.8 | 1.4 | 3.8 | 10 |
| Carbonate cement (%) | 9.4 | 12.3 | 0 | 40 | 19 |
| Intergranular porosity (%) | 11 | 4.6 | 1.7 | 20.7 | 19 |
| Intragranular porosity (%) | 3.3 | 1.5 | 1 | 8 | 19 |
| Core Porosity (%) | 22 | 5.2 | 8.5 | 27.9 | 33 |
| Total clay (%) | 2.8 | 2.3 | 0.7 | 9.3 | 19 |

analyses are shown as a function of the distance from the detrital grain boundary in Fig. 7. All $\delta^{18}O_{(quartz\ cement)}$ values fall within a 2.7‰ range, from +19.7 to +22.4‰ V-SMOW (Fig. 7); the $\delta^{18}O$ values from all three overgrowths overlap and there is no trend from grain boundary to cement edge, and no relationship to concentric CL zonation.

## 6. Controls on quartz cementation

It is commonly assumed that the rate-controlling step for quartz cementation of sandstones is the precipitation of silica (Ajdukiewicz and Lander, 2010; Walderhaug, 1994a, 1996). In this scenario, the kinetic barriers which inhibit quartz precipitation are overcome, on geological timescales, at temperatures around 70–80 °C (McBride, 1989; Walderhaug, 1994a; Worden and Morad, 2000), above which rates of precipitation increase exponentially with temperature (Walderhaug, 1996). Models using these commonly-used precipitation kinetics predict that sandstones which, like those in Elgin, are buried to *ca*. 190 °C and have experienced temperatures greater than 80 °C for about 90 Myrs, would be very extensively cemented with quartz; however, samples in this study only have an average macroquartz cement content of 4.6 ± 1.2 vol %. Previous studies (Osborne and Swarbrick, 1999; Taylor et al., 2015) have also reported the presence of low volumes of macroquartz cement in other Central North Sea HPHT sandstones. While Osborne and Swarbrick (1999) attributed the lack of quartz cement mainly to the effect of low VES induced by overpressure, Taylor et al. (2015) concluded that the effect of overpressure is insignificant, and that grain coatings are by far the most important factor. In this section, we provide a critical assessment of the controls on quartz cementation in these Fulmar sandstones and offer the best explanation for the occurrence of the small volumes of macroquartz cement.

### 6.1. Feldspar dissolution

Sandstones in this study are rich in feldspar, especially K-feldspars and some plagioclase. Partially or completely dissolved feldspars with initial shapes preserved as moldic pores are common in Upper Jurassic Fulmar sandstones (Osborne and Swarbrick, 1999; Taylor et al., 2015; Wilkinson and Haszeldine, 1996) and were also observed in this study (Fig. 4C and D). Feldspar dissolution as a mid to late diagenetic process in deeply-buried Upper Jurassic Fulmar Formation has a profound, positive effect on reservoir quality (Lasocki et al., 1999; Wilkinson et al., 1997). Reaction products of feldspar dissolution include illite, which may be deposited in adjacent intergranular pores (Giles, 1987; Taylor et al., 2015), and silica (Osborne and Swarbrick, 1999; Worden and Morad, 2000) which may precipitate as macroquartz cements.

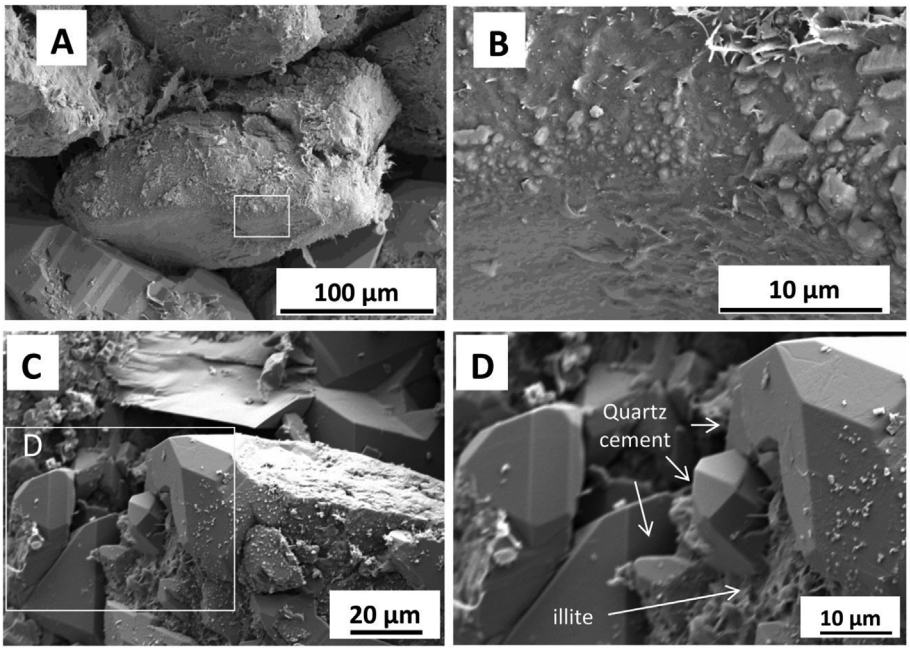


**Fig. 5.** SEM images of Upper Jurassic Fulmar Formation sandstones from Elgin field. A) Low magnification of a quartz grain surface with limited clay and microquartz coatings. B) High magnification corresponding to the box in Plate A showing poorly developed microquartz overgrowth and clay coats. Microquartz overgrowths are very uncommon in this study. C) Low magnification SEM image of quartz grains with macroquartz cement. D) Higher magnification image corresponding to the box in Plate C showing that the presence of poorly-developed illite coatings did not prevent the growth of macroquartz.

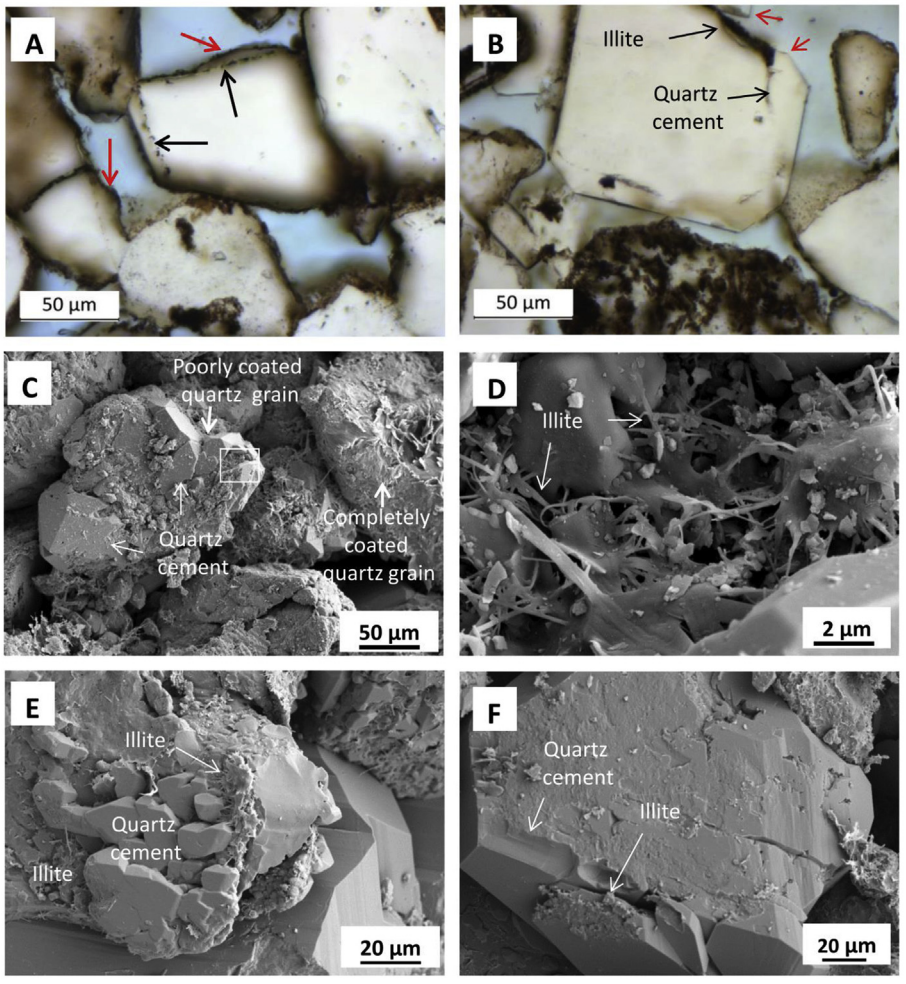


**Fig. 6.** Micrographs of Upper Jurassic Fulmar Formation sandstones from Elgin field. A) Bitumen-stained illite with later quartz cement (black arrow); bitumen-impregnated authigenic illite (red arrows) coating earlier quartz cement surfaces. B) Quartz cements (red arrows) projecting over incomplete, bitumen-stained illite coatings. C) Quartz grain with quartz cement adjacent to another grain lacking quartz cement due to complete illite coatings. D) High magnification image corresponding to the box in Plate C. E) Quartz cement nucleation on detrital grain with poorly-developed illite coatings. F) Later illite formed on quartz cement. (For interpretation of the references to colour in this figure legend, the reader is referred to the Web version of this article.)

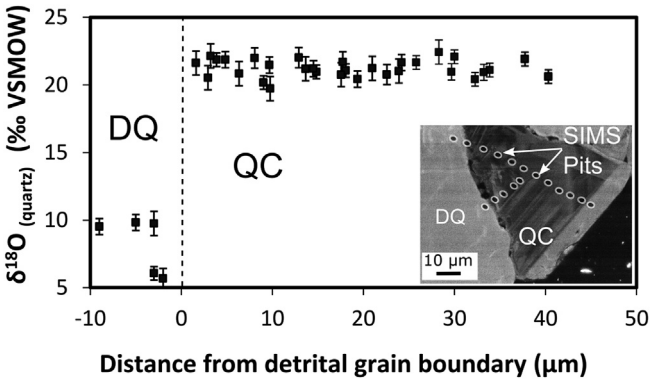


**Fig. 7.** Plot of $\delta^{18}O$ of quartz cement (QC) and detrital quartz (DQ) against distance in microns from detrital grain boundary for three quartz overgrowths. The inset CL micrograph shows one of the three analysed overgrowths. The CL image shows 3 µm diameter ion microprobe sampling spots (SIMS pits).

Petrographic data from modal analysis of thin sections reveals intragranular porosity from feldspar dissolution makes up about 3.3% of bulk rock volume in the analysed samples. These data were used to estimate the volume of illite (Osborne and Swarbrick, 1999) and silica contributed to the system as a result of feldspar dissolution. In this study, silica from feldspar dissolution is a significant fraction of that observed as macroquartz cement. Writing the conversion of K-feldspar to illite as:

$$1.0\ \text{K-feldspar} + 0.174H2O + 0.522\ H+ + 0.109\ Mg^{2}+ = 0.739\ K+ + 0.435\ \text{Illite} + 1.478\ \text{Quartz},$$

and using the amount of illite (2.8%) observed in these samples as a reaction product, we estimate that dissolved feldspars supplied around 25% of the silica occurring as macroquartz cement.

### 6.2. Grain-coating microquartz

The occurrence of early, grain-coating microquartz on detrital quartz has been described as an effective inhibitor of macroquartz cementation in deeply-buried sandstones (e.g. Aase et al. (1996)). For example, sponge spicules from organisms such as *Rhaxella* dissolve at low temperatures and reprecipitate on clean detrital quartz surfaces as tiny, microcrystalline quartz overgrowths (Aase et al., 1996; Osborne and Swarbrick, 1999). Various mechanisms have been proposed to explain the way in which grain-coating microquartz inhibits the development of macroquartz cements: first, by inhibiting intergranular pressure solution through maintaining a higher equilibrium activity of dissolved silica as a result of the higher solubility of microquartz; and second, by arresting both mechanical and chemical compaction/pressure dissolution through the early formation of a rigid framework structure due to microquartz precipitation (Aase et al., 1996; Osborne and Swarbrick, 1999). Recent studies (French and Worden, 2013; French et al., 2012; Worden et al., 2012) have, however, identified that an amorphous silica layer usually exists between quartz grains and microcrystalline quartz overgrowths that not only give the overlying microcrystalline quartz their random orientation, but also insulates the host grain from macroquartz precipitation.

Several studies (Aase et al., 1996; Gowland, 1996; Osborne and Swarbrick, 1999; Stewart, 1986; Taylor et al., 2015) have documented the occurrence of sponge spicules and microquartz overgrowths within some stratigraphic intervals in the Upper Jurassic Fulmar and other Mesozoic sandstones in the Central North Sea. However, detailed transmitted and SEM analysis shows that grain-coating microquartz cements are rare in our sample set (Fig. 5A and B). Sparse and incomplete microquartz overgrowths were also reported by Taylor et al. (2015) in the Fulmar sandstones from Shearwater field, about 6 km to the east of Elgin. We conclude that microquartz cements cannot be responsible for the low volume of macroquartz cement.

### 6.3. Grain-coating clays

The grain-coating effect of clay minerals as an inhibitor of macroquartz cementation has been well documented by several authors (Berger et al., 2009; Bloch et al., 2002; Heald and Larese, 1974; Morad et al., 2010; Nguyen et al., 2013; Stricker et al., 2016a). Authigenic chlorite-coats are the most important and effective inhibitor of macroquartz cementation (Dowey et al., 2012; Ehrenberg, 1993; Taylor et al., 2010). The grain-coating ability of illite has also been reported, though less frequently than chlorite (Storvoll et al., 2002; Taylor et al., 2010). Numerous studies (Osborne and Swarbrick, 1999; Taylor et al., 2015; Wilkinson et al., 1997; Wilkinson and Haszeldine, 1996, 2011) have shown that illite is by far the most common authigenic clay in the Upper Jurassic Fulmar Formation. Previous studies (e.g. Taylor et al., 2015; Wilkinson and Haszeldine, 1996) have shown that authigenic illite precipitates as one of the products of feldspar dissolution in the Upper Jurassic Fulmar Formation. If feldspar dissolution in the Upper Jurassic Fulmar Formation occurred during middle - late diagenesis (Haszeldine et al., 1999; Lasocki et al., 1999; Wilkinson and Haszeldine, 2011), it follows that dissolution-sourced authigenic illite first developed around the same time and temperature. Since the macroquartz cementation threshold is around 70–80 °C (e.g. Walderhaug, 1994a), some macroquartz cement would have precipitated on free detrital quartz surfaces in the Upper Jurassic Fulmar Formation prior to authigenic illite formation. Evidence from petrographic analysis (Fig. 6A and F) confirms this assertion, as authigenic illite is seen coating the surfaces of some macroquartz overgrowths, suggesting that quartz cementation predates authigenic illite formation.

On the contrary, detrital grain-coating clays (Taylor et al., 2015; Wilkinson and Haszeldine, 2011) may exert some inhibitive effect on macroquartz cementation in the Fulmar Formation, although it is difficult to distinguish detrital illite from authigenic illite as a result of their diagenetic recrystallization (Wilkinson and Haszeldine, 2011). In this study, illite most commonly coats less than 30% of quartz surfaces (Fig. 8). The effect of these poorly developed grain-coats is that macroquartz cement often nucleates on the host detrital quartz due to breaks in coat continuity (Fig. 5C and D and Fig. 6). Quartz cements also engulf some grain-coating illite (Fig. 6A). The implication is that discontinuous coats are not a very effective brake on quartz cementation. In order to test this claim, we incorporated clay coat data into the quartz cementation model used for this study. The model (Fig. 9) suggests that even 50% clay coat coverage for the detrital quartz fraction

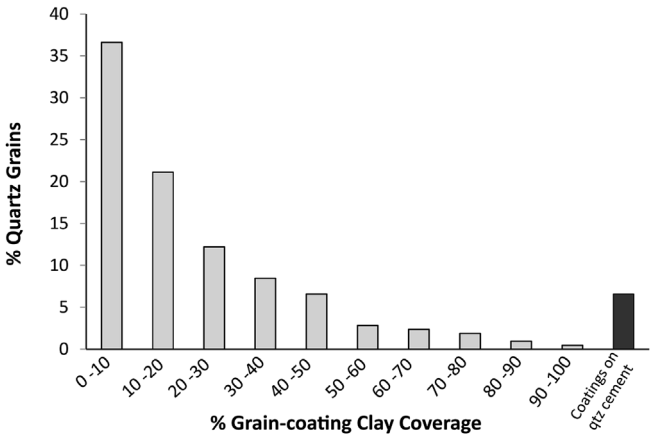


**Fig. 8.** Percentage of quartz grains in analysed Fulmar Formation samples with their corresponding percentage grain-coating clay coverage. Black bar represents percentage of authigenic quartz (overgrowths) with clay coats.

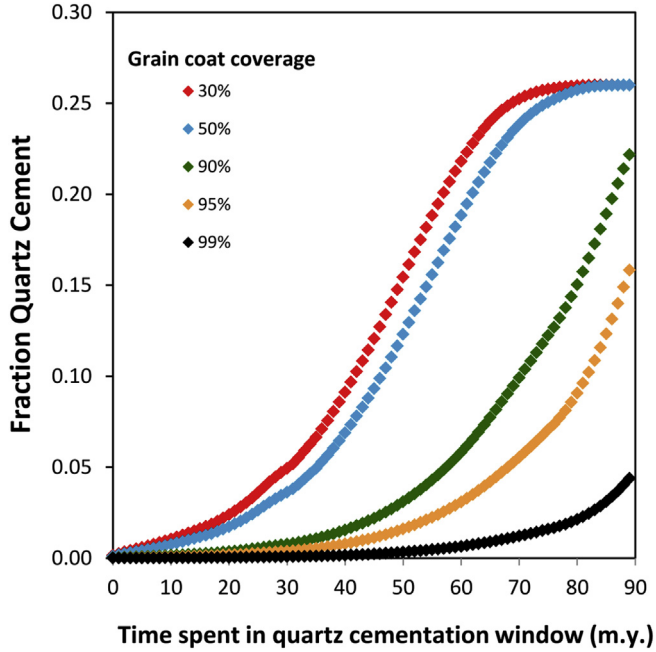


**Fig. 9.** Quartz cementation model output for Upper Jurassic Fulmar Formation sandstones from Elgin field showing evolution of quartz cement through geologic time. Walderhaug's (1996) approach was applied to 1 $cm^3$ volume of the studied sandstone using an 80 °C threshold temperature for cementation and a starting porosity of 26%. Time-temperature history was generated using PetroMod version 2014.1. The model also tested different grain coat coverage scenarios ranging from 30 to 99%, and the outputs suggest that the studied sandstones would require around 99% grain coat coverage for their present average quartz cement volume (4.6%). In order to incorporate the grain coat data in the model, the initial quartz surface area was reduced using the estimated grain coatings coverage area.

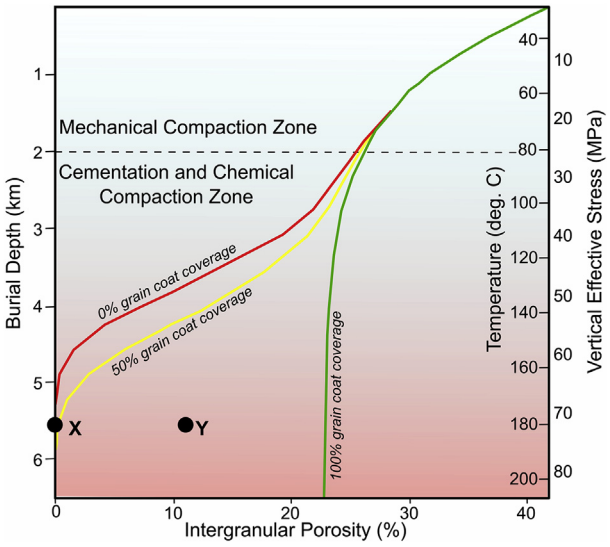


**Fig. 10.** Modified, hypothetical plot of porosity-depth trends with burial process and lithology based on Ajdukiewicz and Lander (2010). The well-sorted, fine-grained arkosic eolian sandstone assumed in this model has a simple burial history, variable grain coat coverage from shallow depth, and zero overpressure. Projection of the analysed Fulmar Formation sandstones on the plot based on burial depth, temperature, and average grain coat coverage (X) suggests that the sandstones should be completely cemented at Present-day. However, the measured average intergranular porosity in the sandstones (Y) is 11%.

would have little or no effect on quartz cementation. Similarly, comparison with Ajdukiewicz and Lander's (2010) porosity-depth/temperature model, in which quartz cementation is modelled using an Arrhenius approach, suggests that sandstones at 190 °C should be completely cemented at the level of grain coat coverage observed in this study (Fig. 10). The model was subsequently tested by varying the clay coat coverage values. The concurrence between measured and modelled quartz cement volume was achieved around 99% clay coat coverage (Fig. 9). A simplified interpretation for these data would mean that each detrital quartz grain must be almost completely coated (99%) in order to limit the average volume of quartz cement to the observed value (4.6%).

In addition, some studies (Fisher et al., 2009; Harris, 2006) have shown that detrital and authigenic illite at detrital quartz intergranular contacts behaves like other sheet silicates (e.g. micas) by promoting dissolution and subsequently increasing the local supply of silica for macroquartz cementation.

Overall, grain-coating illite has only had limited influence on quartz cementation in the Fulmar Formation; their limited distribution means that they cannot account for the low volume of quartz cement in the studied HPHT sandstones.

### 6.4. Hydrocarbon emplacement

The role of hydrocarbon emplacement on macroquartz cementation in deeply buried sandstones has long been a subject of controversy. As a result, two schools of thought exist in the literature: those who suggest that early hydrocarbon emplacement can inhibit macroquartz cementation (Dixon et al., 1989; Emery et al., 1993; Gluyas et al., 1993; Haszeldine et al., 2003; Marchand et al., 2000, 2001, 2002; Saigal et al., 1992; Wilkinson and Haszeldine, 2011; Worden et al., 1998, 2018a, 2018b) and those who reported that hydrocarbon charge exerts no significant effect (Aase et al., 1996; Aase and Walderhaug, 2005; Molenaar et al., 2008). In general, field (Maast et al., 2011; Marchand et al., 2002; Worden et al., 1998, 2018b) and experimental (Sathar et al., 2012) observations suggest that early hydrocarbon charge, high hydrocarbon saturation and an oil-wet reservoir are required if hydrocarbons are to effectively halt the macroquartz cementation process.

Elgin is of course a hydrocarbon-filled reservoir and we can observe bitumen-impregnated illite coating some detrital quartz grains and overgrowths (Fig. 6A and F). In the context of quartz cementation, it is therefore important to establish the timing of hydrocarbon charge. The reconstruction of the thermal history of the Elgin horst structure shows that expulsion started from local source rocks in the Eocene. This result was however treated with caution because (1) we used a one dimensional model that considers only the source rocks on the Elgin horst structure, which may not be the main source of the petroleum in the Fulmar Formation reservoir (Rudkiewicz et al., 2000), and (2) organic geochemistry data suggest that the oil and condensates in the Fulmar Formation reservoir in Elgin are high maturity fluids that are mostly sourced from the Kimmeridge Clay and Heather Formations in the deeper part of the Central Graben (Isaksen, 2004). The hydrocarbon charge history, as constrained by Rudkiewicz et al. (2000) using a three-dimensional basin model incorporating the deeper source rocks, also shows an Eocene arrival time (38 Ma). This implies that the Fulmar Formation in Elgin field would have been in the quartz cementation window for over 50 Myrs (Fig. 3) prior to significant hydrocarbon charge, and that substantial macroquartz cement would still have precipitated in the Fulmar Formation reservoir during burial between the onset of macroquartz cementation (80 °C) to the time of hydrocarbon charge (135 °C). Prior to being charged, hydrocarbon saturation and wetting state are of course irrelevant as inhibitors of quartz cementation.

This result is consistent with Hendry et al.'s, (2000) study that suggests hydrocarbon emplacement post-dates the precipitation of ankerite cements (140–170 °C) in the Elgin field. Oil-impregnation of illite

grain-coats most probably occurred at high temperatures and thus played little role in inhibiting macroquartz cementation.

### 6.5. Vertical effective stress

Vertical effective stress is the stress exerted on a layer of rock by the weight of overlying sediment or overburden. The role of vertical effective stress as an effective driver of intergranular pressure dissolution and chemical compaction has been well documented (De Boer et al., 1977; Dewers and Ortoleva, 1990, 1991; Elias and Hajash, 1992; Gratier et al., 2005; Nenna and Aydin, 2011; Renard et al., 1997, 1999; Robin, 1978; Rutter and Elliott, 1976; Sheldon et al., 2003; Shimizu, 1995; Tada et al., 1987; Tada and Siever, 1989; Thomson, 1959; van Noort et al., 2008; Weyl, 1959). The magnitude of vertical effective stress in a sedimentary system is dependent on the pore pressure regime, such that an increase or decrease in pore pressure would produce a corresponding decrease or increase in vertical effective stress (Osborne and Swarbrick, 1999). Theoretical (Sheldon et al., 2003), experimental (Elias and Hajash, 1992; Gratier et al., 2005; van Noort et al., 2008) and field-based (Houseknecht, 1988; Thomson, 1959) evidence shows that intergranular pressure dissolution occurs in response to the development of anisotropic stress in sandstones. The presence of sheet silicates only helps to catalyse the process by influencing the rate of dissolution and diffusion (Sheldon et al., 2003). Previous experimental studies on compaction in granular quartz (De Boer et al., 1977; Elias and Hajash, 1992; Gratier et al., 2005; Niemeijer et al., 2002; Rutter and Elliott, 1976; van Noort et al., 2008) showed that the rate of chemical compaction of quartz-rich sandstones at depth > 2500 m is indeed sensitive to temperature changes, but that the process is primarily controlled by stress-induced, pressure dissolution. Since chemical compaction is stress-sensitive, high pore fluid pressures would arrest the driving force for intergranular pressure dissolution and chemical compaction by limiting the vertical effective stress; by limiting the source of silica, this would in turn reduce the rate of macroquartz cementation (Ehrenberg, 1990; Osborne and Swarbrick, 1999; Sheldon et al., 2003; Stricker et al., 2016b), largely independent of the prevailing temperature regime.

Basin modelling suggests that the initiation of a continuous phase of overpressure development in the Elgin area started in the early Upper Cretaceous (95 Ma) through to the present-day, and that VES has never been greater than the present value of 12.5 MPa. The continuously low VES basin modelling result is consistent with petrographic observations such as the presence of uncollapsed, moldic pores (Fig. 4C and D) and the absence of sutured or stylolitic grain contacts.

Whilst few dispute the role of intergranular pressure dissolution as a source of silica and thus of macroquartz cement in sandstones, the strong, current consensus is that the rate of macroquartz cementation in sandstones is a primary function of temperature-controlled quartz precipitation kinetics (Bjorkum, 1996; Taylor et al., 2015; Walderhaug, 1994b). An alternative view was proposed by Osborne and Swarbrick (1999), who argued that rates of intergranular pressure dissolution were influenced by vertical effective stress. Our data support that assertion, to the extent that we argue that vertical effective stress is the main control on macroquartz cementation in Elgin's Fulmar Formation sandstones. Vertical effective stress has never been more than ca. 12.5 MPa throughout the burial history of the Fulmar sands, so that despite the fact that (a) the present-day temperature is 190 °C and (b) the Fulmar sands have spent > 90 Ma in the > 70–80 °C "quartz cementation window", the supply of silica at grain-grain contacts has been restricted by the continuing occurrence of high fluid pressures/low vertical effective stresses.

Notably, a lack of correlation between macroquartz cement volume and intergranular pressure dissolution has been cited elsewhere as evidence for non-suppression of macroquartz cementation by high fluid pressure/low vertical effective stress (e.g. Taylor et al., 2015). Because an overpressured system is essentially closed, diagenesis in such systems is limited to that possible within the realm of their indigenous fluid chemistry (Jeans, 1994; Stricker et al., 2016a). The implication is that the observed macroquartz cements in the studied sandstones were most likely sourced locally. CL petrography shows that intergranular pressure dissolution can source 60–70% of the silica for the observed macroquartz cement, with the rest likely supplied by feldspar dissolution (Fig. 11).

### 6.6. Quartz cementation history

We now argue that *in situ* $\delta^{18}O_{quartz\ cement}$ profiles across individual overgrowths support our interpretation that macroquartz cement occurred over a wide temperature range, which in turn supports the interpretation that the rate of macroquartz cementation was both slow and controlled by the rate of silica supply, not precipitation. *In situ* oxygen isotopic profiles across three individual overgrowths exhibit a total range of 2.7‰, between 22.4 and 19.7‰ (Fig. 7). Since the oxygen isotopic composition of quartz is a dual function of temperature and $\delta^{18}O_{H2O}$, the $\delta^{18}O_{quartz\ cement}$ data cannot generate a unique temperature record of macroquartz precipitation. We can however propose the most geologically realistic interpretation of the isotope data (Fig. 12). We first reject the model that macroquartz precipitated from a water of constant $\delta^{18}O$ between 80 and 190 °C, since $\delta^{18}O_{quartz\ cement}$ would then exhibit a 12‰ range. Secondly, if macroquartz precipitation started at 80 °C with a $\delta^{18}O_{quartz\ cement}$ value of +22.4‰, then it would have done so from a fluid similar to that of Jurassic seawater (−1‰). If all of the macroquartz precipitated from Jurassic seawater, then all cementation would have occurred between 80 and 100 °C, which is extremely unlikely given the many studies (e.g. Walderhaug, 1994a; 1994b) which have shown that macroquartz cementation continues to much higher temperatures. Most likely, we suggest, is that because the present-day $\delta^{18}O_{H2O}$ in local Fulmar Formation sandstones is +4.5‰ (Hendry et al., 2000), $\delta^{18}O_{H2O}$ evolved from −1 to +4.5‰ during the period of macroquartz precipitation, giving a temperature window of 80–150 °C (Fig. 12). We suggest that the lack of an isotopic record for temperatures beyond 150 °C was probably due to the subsequent high degree of hydrocarbon saturation from charging of the Fulmar Formation reservoir from the deeper source kitchen. We therefore suggest that this is the most reasonable explanation of the $\delta^{18}O_{quartz\ cement}$ data, being consistent with what is generally inferred about the onset of macroquartz cementation and also with what is known about the most probable diagenetic fluids in Elgin and the way that $\delta^{18}O_{H2O}$ tends to evolve, to heavier values, during burial diagenesis (Aplin and Warren, 1994; Warren et al., 1994). Using an 80–150 °C window for macroquartz cementation, and taking into account the potential inhibiting effects of clay coats, the kinetic model for quartz precipitation would then predict 25 vol % macroquartz cement, compared with the actual 4.6% (Figs. 9 and 10).

These data, combined with (a) the long history of low vertical effective stress and (b) the lack of any other factors which would significantly inhibit quartz precipitation, strongly suggest that macroquartz cementation is controlled by the stress-related supply of silica at grain-grain contacts and *not* by precipitation kinetics at free quartz surfaces.

The lack of a volumetrically significant amount of macroquartz cement in the studied sandstones at their current burial depth and temperature (190 °C) contrasts with observations made for other deeply buried sandstones like the Garn Formation in the North Sea (Giles et al., 1992; Osborne and Swarbrick, 1999) and the Wilcox sandstones in the Gulf of Mexico (Dutton and Loucks, 2010), where large volumes of macroquartz cement are seen at high temperatures. This study has strong implications for the role of temperature and stress in the entire macroquartz cementation process. While temperature is an important control on quartz precipitation kinetics, substantial volumes of macroquartz cement cannot develop if the supply of silica (source) is cut-off or greatly reduced.

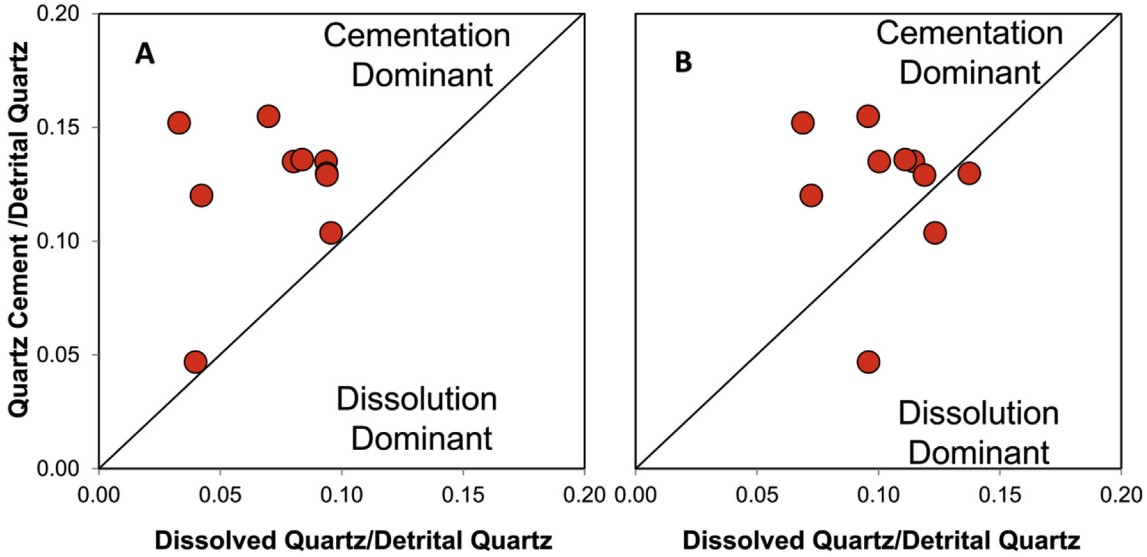


**Fig. 11.** Plot of Fulmar Formation sandstones silica budget generated from petrographic data. All data have been normalised to detrital quartz content. A) Quantified pressure dissolution, represented by overlap quartz, supplied around 60% of the silica for precipitation of quartz cement. B) The incorporation of silica generated from feldspar dissolution into the budget analysis suggests feldspar dissolution and intergranular pressure dissolution can supply most or all the silica for quartz cementation from local sources.

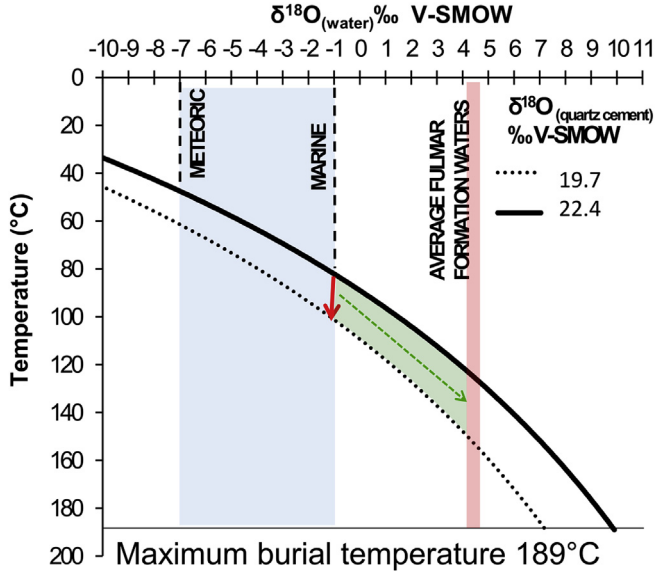


**Fig. 12.** Plot of $\delta^{18}O_{(water)}$ in equilibrium with $\delta^{18}O_{(quartz\ cement)}$ as a function of temperature (Clayton et al., 1972). $\delta^{18}O_{(quartz\ cement)}$ contours 19.7 and 22.4‰ VSMOW defines the $\delta^{18}O$ range from early to late quartz cement. The red arrow represents an unlikely pathway for quartz cement precipitation, since $\delta^{18}O_{(water)}$ evolved to Present-day Formation water values (~4.5‰) in the Fulmar Formation reservoir (green arrow). (For interpretation of the references to colour in this figure legend, the reader is referred to the Web version of this article.)

## 7. Conclusions

Fulmar Formation sandstones buried to 190 °C in the Elgin field have very low volumes of quartz cement. This contrasts with many other deeply buried sandstones where large volumes of quartz cements are present at high temperatures. Neither grain-coating microquartz nor illite can account for the low volume of quartz cement. Charge history reconstruction shows that hydrocarbons arrived at a temperature at which significant quartz cement would have already formed, so that hydrocarbon emplacement cannot be the cause of the low volume of quartz cement. Since basin modelling suggests that vertical effective stress was low throughout the burial history of these sands, we suggest that the rate of intergranular pressure dissolution was restricted by the continuously low vertical effective stress; it is therefore the rate of silica supply from intergranular pressure dissolution, not the rate of precipitation, which is the main control of quartz cementation. This is supported by *in situ* oxygen isotope analyses across individual quartz overgrowths which suggest that quartz cement formed over 100 Ma at an exceptionally slow rate, between 80 and 150 °C.

## Acknowledgements

Petroleum Technology Development Fund, Nigeria is thanked for funding this research. We acknowledge support from BGS for access to core material, and IHS for access to data from Central North Sea wells. The WiscSIMS Lab is supported by the US National Science Foundation (Ear-1658823) and the University of Wisconsin-Madison. JWV is supported by the US Department of Energy, Office of Basic Energy Sciences, Chemical Sciences, Geosciences, and Biosciences Division (DE-FG02-93ER14389). Richard Worden and Mark Osborne are thanked for their constructive and helpful reviews.

## Appendix A. Supplementary data

Supplementary data to this article can be found online at https://doi.org/10.1016/j.marpetgeo.2018.09.017.

## References

Aase, N.E., Bjorkum, P.A., Nadeau, P.H., 1996. The effect of grain-coating microquartz on preservation of reservoir porosity. AAPG (Am. Assoc. Pet. Geol.) Bull. 80, 1654–1673.
Aase, N.E., Walderhaug, O., 2005. The effect of hydrocarbons on quartz cementation: diagenesis in the Upper Jurassic sandstones of the Miller Field, North Sea, revisited. Petrol. Geosci. 11, 215–223.
Ajdukiewicz, J., Nicholson, P., Esch, W., 2010. Prediction of deep reservoir quality using early diagenetic process models in the Jurassic Norphlet Formation, Gulf of Mexico. AAPG (Am. Assoc. Pet. Geol.) Bull. 94, 1189–1227.
Ajdukiewicz, J.M., Lander, R.H., 2010. Sandstone reservoir quality prediction: the state of the art. AAPG (Am. Assoc. Pet. Geol.) Bull. 94, 1083–1091.
Allen, P.A., Allen, J.R., 2005. Basins Due to Lithospheric Stretching, Basin Analysis: Principles and Applications, second ed. Blackwell Publishing, Australia, pp. 63–115.
Aplin, A.C., Warren, E.A., 1994. Oxygen isotopic indications of the mechanisms of silica transport and quartz cementation in deeply buried sandstones. Geology 22, 847–850.
Berger, A., Gier, S., Krois, P., 2009. Porosity-preserving chlorite cements in shallow-marine volcaniclastic sandstones: evidence from Cretaceous sandstones of the Sawan

gas field, Pakistan. AAPG (Am. Assoc. Pet. Geol.) Bull. 93, 595–615.
Bjorkum, P.A., 1996. How important is pressure in causing dissolution of quartz in sandstones? J. Sediment. Res. 66, 147–154.
Bjørkum, P.A., Oelkers, E.H., Nadeau, P.H., Walderhaug, O., Murphy, W.M., 1998. Porosity prediction in quartzose sandstones as a function of time, temperature, depth, stylolite frequency, and hydrocarbon saturation. AAPG (Am. Assoc. Pet. Geol.) Bull. 82, 637–648.
Bloch, S., Lander, R.H., Bonnell, L., 2002. Anomalously high porosity and permeability in deeply buried sandstone reservoirs: origin and predictability. AAPG (Am. Assoc. Pet. Geol.) Bull. 86, 301–328.
Clayton, R.N., O'Neil, J.R., Mayeda, T.K., 1972. Oxygen isotope exchange between quartz and water. J. Geophys. Res. 77, 3057–3067.
Darby, D., Haszeldine, R.S., Couples, G.D., 1996. Pressure cells and pressure seals in the UK Central Graben. Mar. Petrol. Geol. 13, 865–878.
De Boer, R., Nagtegaal, P., Duyvis, E., 1977. Pressure solution experiments on quartz sand. Geochim. Cosmochim. Acta 41, 257–264.
Dewers, T., Ortoleva, P., 1990. A coupled reaction/transport/mechanical model for intergranular pressure solution, stylolites, and differential compaction and cementation in clean sandstones. Geochim. Cosmochim. Acta 54, 1609–1625.
Dewers, T., Ortoleva, P., 1991. Influences of clay minerals on sandstone cementation and pressure solution. Geology 19, 1045–1048.
Dixon, S., Summers, D., Surdam, R., 1989. Diagenesis and preservation of porosity in norphlet formation (upper Jurassic), southern Alabama. AAPG (Am. Assoc. Pet. Geol.) Bull. 73, 707–728.
Dowey, P.J., Hodgson, D.M., Worden, R.H., 2012. Pre-requisites, processes, and prediction of chlorite grain coatings in petroleum reservoirs: a review of subsurface examples. Mar. Petrol. Geol. 32, 63–75.
Dutton, S.P., Loucks, R.G., 2010. Diagenetic controls on evolution of porosity and permeability in lower Tertiary Wilcox sandstones from shallow to ultradeep (200–6700m) burial, Gulf of Mexico Basin, USA. Mar. Petrol. Geol. 27, 69–81.
Eggink, J., Riegstra, D., Suzanne, P., 1996. Using 3D seismic to understand the structural evolution of the UK Central North Sea. Petrol. Geosci. 2, 83–96.
Ehrenberg, S., 1990. Relationship between diagenesis and reservoir quality in sandstones of the Garn Formation, Haltenbanken, mid-Norwegian continental shelf (1). AAPG (Am. Assoc. Pet. Geol.) Bull. 74, 1538–1558.
Ehrenberg, S., 1993. Preservation of anomalously high porosity in deeply buried sandstones by grain-coating chlorite: examples from the Norwegian continental shelf. AAPG (Am. Assoc. Pet. Geol.) Bull. 77, 1260–1286.
Elias, B.P., Hajash, A., 1992. Changes in quartz solubility and porosity due to effective stress: an experimental investigation of pressure solution. Geology 20, 451–454.
Emery, D., Smalley, P., Oxtoby, N., Ragnarsdottir, K., Aagaard, P., Halliday, A., Coleman, M., Petrovich, R., 1993. Synchronous oil migration and cementation in sandstone reservoirs demonstrated by quantitative description of diagenesis. Phil. Trans. Roy. Soc. Lond.: Math. Phys. Eng. Sci. 344, 115–125.
Evans, J., Hogg, A.J., Hopkins, M.S., Howarth, R.J., 1994. Quantification of quartz cements using combined SEM, CL, and image analysis. J. Sediment. Res. 64, 334–338.
Fisher, Q., Knipe, R., Worden, R., 2009. Microstructures of deformed and non-deformed sandstones from the North Sea: implications for the origins of quartz cement in sandstones. In: In: Worden, R., Morad, S. (Eds.), Quartz Cementation in Sandstones, vol. 2009. John Wiley & Sons, pp. 129–146.
French, M.W., Worden, R.H., 2013. Orientation of microcrystalline quartz in the Fontainebleau Formation, Paris Basin and why it preserves porosity. Sediment. Geol. 284, 149–158.
French, M.W., Worden, R.H., Mariani, E., Larese, R.E., Mueller, R.R., Kliewer, C.E., 2012. Microcrystalline quartz generation and the preservation of porosity in sandstones: evidence from the upper Cretaceous of the Subhercynian basin, Germany. J. Sediment. Res. 82, 422–434.
Giles, M., 1987. Mass transfer and problems of secondary porosity creation in deeply buried hydrocarbon reservoirs. Mar. Petrol. Geol. 4, 188–204.
Giles, M., Stevenson, S., Martin, S., Cannon, S., Hamilton, P., Marshall, J., Samways, G., 1992. The reservoir properties and diagenesis of the Brent Group: a regional perspective. Geol. Soc., London 61, 289–327 Special Publications.
Gluyas, J., Robinson, A., Emery, D., Grant, S., Oxtoby, N., 1993. The link between petroleum emplacement and sandstone cementation. In: Geological Society, London, Petroleum Geology Conference Series. Geological Society of London, pp. 1395–1402.
Gluyas, J.G., Hichens, H.M., 2003. United Kingdom Oil and Gas Fields: Commemorative Millennium Volume. Geological Society of London, pp. 485–647 41-44.
Gowland, S., 1996. Facies Characteristics and Depositional Models of Highly Bioturbated Shallow Marine Siliciclastic Strata: an Example from the Fulmar Formation (Late Jurassic), UK Central Graben. vol. 114. Geological Society, London, Special Publications, pp. 185–214.
Gratier, J.-P., Muquet, L., Hassani, R., Renard, F., 2005. Experimental microstylolites in quartz and modeled application to natural stylolitic structures. J. Struct. Geol. 27, 89–100.
Harris, N.B., 2006. Low-porosity haloes at stylolites in the feldspathic Upper Jurassic Ula sandstone, Norwegian North Sea: an integrated petrographic and chemical mass-balance approach. J. Sediment. Res. 76, 444–459.
Harwood, J., Aplin, A.C., Fialips, C.I., Iliffe, J.E., Kozdon, R., Ushikubo, T., Valley, J.W., 2013. Quartz cementation history of sandstones revealed by high-resolution Sims oxygen isotope analysis. J. Sediment. Res. 83, 522–530.
Haszeldine, R., Wilkinson, M., Darby, D., Macaulay, C., Couples, G., Fallick, A., Fleming, C., Stewart, R., McAulay, G., 1999. Diagenetic Porosity Creation in an Overpressured Graben, Geological Society, London, Petroleum Geology Conference Series. Geological Society of London, pp. 1339–1350.
Haszeldine, R.S., Cavanagh, A.J., England, G.L., 2003. Effects of oil charge on illite dates and stopping quartz cement: calibration of basin models. J. Geochem. Explor. 78, 373–376.
Heald, M., Larese, R., 1974. Influence of coatings on quartz cementation. J. Sediment. Res. 44, 1269–1274.
Hendry, J.P., Wilkinson, M., Fallick, A.E., Haszeldine, R.S., 2000. Ankerite cementation in deeply buried Jurassic sandstone reservoirs of the central North Sea. J. Sediment. Res. 70, 227–239.
Houseknecht, D.W., 1988. Intergranular pressure solution in four quartzose sandstones. J. Sediment. Res. 58, 228–246.
Houseknecht, D.W., 1991. Use of Cathodoluminescence Petrography for Understanding Compaction, Quartz Cementation, and Porosity in Sandstones. SEPM Special Publication SC25, pp. 59–66.
Isaksen, G.H., 2004. Central North Sea hydrocarbon systems: generation, migration, entrapment, and thermal degradation of oil and gas. AAPG (Am. Assoc. Pet. Geol.) Bull. 88, 1545–1572.
Jeans, C., 1994. Clay diagenesis, overpressure and reservoir quality: an introduction. Clay Miner. 29, 415–424.
Kelly, J.L., Fu, B., Kita, N.T., Valley, J.W., 2007. Optically continuous silcrete quartz cements of the St. Peter Sandstone: high precision oxygen isotope analysis by ion microprobe. Geochim. Cosmochim. Acta 71, 3812–3832.
Kita, N.T., Ushikubo, T., Fu, B., Valley, J.W., 2009. High precision SIMS oxygen isotope analysis and the effect of sample topography. Chem. Geol. 264, 43–57.
Lander, R.H., Walderhaug, O., 1999. Predicting porosity through simulating sandstone compaction and quartz cementation. AAPG (Am. Assoc. Pet. Geol.) Bull. 83, 433–449.
Lasocki, J., Guemene, J., Hedayati, A., Legorjus, C., Page, W., 1999. The Elgin and Franklin Fields: UK Blocks 22/30c, 22/30b and 29/5b, Geological Society, London, Petroleum Geology Conference Series. Geological Society of London, pp. 1007–1020.
Maast, T.E., Jahren, J., Bjorlykke, K., 2011. Diagenetic controls on reservoir quality in middle to upper Jurassic sandstones in the south Viking Graben, North Sea. AAPG (Am. Assoc. Pet. Geol.) Bull. 95, 1937–1958.
Marchand, A., Haszeldine, R., Macaulay, C., Swennen, R., Fallick, A., 2000. Quartz cementation inhibited by crestal oil charge: miller deep water sandstone, UK North Sea. Clay Miner. 35 201-201.
Marchand, A.M., Haszeldine, R.S., Smalley, P.C., Macaulay, C.I., Fallick, A.E., 2001. Evidence for reduced quartz-cementation rates in oil-filled sandstones. Geology 29, 915–918.
Marchand, A.M., Smalley, P.C., Haszeldine, R.S., Fallick, A.E., 2002. Note on the importance of hydrocarbon fill for reservoir quality prediction in sandstones. AAPG (Am. Assoc. Pet. Geol.) Bull. 86, 1561–1572.
McBride, E.F., 1989. Quartz cement in sandstones: a review. Earth Sci. Rev. 26, 69–112.
Molenaar, N., Cyziene, J., Sliaupa, S., Craven, J., 2008. Lack of inhibiting effect of oil emplacement on quartz cementation: evidence from Cambrian reservoir sandstones, Paleozoic Baltic Basin. Geol. Soc. Am. Bull. 120, 1280–1295.
Morad, S., Al-Ramadan, K., Ketzer, J.M., De Ros, L., 2010. The impact of diagenesis on the heterogeneity of sandstone reservoirs: a review of the role of depositional facies and sequence stratigraphy. AAPG (Am. Assoc. Pet. Geol.) Bull. 94, 1267–1309.
Nenna, F., Aydin, A., 2011. The formation and growth of pressure solution seams in clastic rocks: a field and analytical study. J. Struct. Geol. 33, 633–643.
Nguyen, B.T., Jones, S.J., Goulty, N.R., Middleton, A.J., Grant, N., Ferguson, A., Bowen, L., 2013. The role of fluid pressure and diagenetic cements for porosity preservation in Triassic fluvial reservoirs of the Central Graben, North Sea. AAPG (Am. Assoc. Pet. Geol.) Bull. 97, 1273–1302.
Nichols, G., 2009. Sedimentology and Stratigraphy. John Wiley & Sons.
Niemeijer, A., Spiers, C., Bos, B., 2002. Compaction creep of quartz sand at 400–600 C: Experimental evidence for dissolution-controlled pressure solution. Earth Planet Sci. Lett. 195, 261–275.
Oelkers, E.H., Bjørkum, P., Murphy, W.M., 1996. A petrographic and computational investigation of quartz cementation and porosity reduction in North Sea sandstones. Am. J. Sci. 296, 420–452.
Osborne, M.J., Swarbrick, R.E., 1999. Diagenesis in North Sea HPHT clastic reservoirs—consequences for porosity and overpressure prediction. Mar. Petrol. Geol. 16, 337–353.
Page, F., Ushikubo, T., Kita, N.T., Riciputi, L., Valley, J.W., 2007. High-precision oxygen isotope analysis of picogram samples reveals 2 μm gradients and slow diffusion in zircon. Am. Mineral. 92, 1772–1775.
Pollington, A.D., Kozdon, R., Valley, J.W., 2011. Evolution of quartz cementation during burial of the cambrian mount Simon sandstone, Illinois basin: in situ microanalysis of $\delta^{18}O$. Geology 39, 1119–1122.
Reilly, M.J., Flemings, P.B., 2010. Deep pore pressures and seafloor venting in the Auger Basin, Gulf of Mexico. Basin Res. 22, 380–397.
Renard, F., Ortoleva, P., Gratier, J.P., 1997. Pressure solution in sandstones: influence of clays and dependence on temperature and stress. Tectonophysics 280, 257–266.
Renard, F., Park, A., Ortoleva, P., Gratier, J.-P., 1999. An integrated model for transitional pressure solution in sandstones. Tectonophysics 312, 97–115.
Robin, P.-Y.F., 1978. Pressure solution at grain-to-grain contacts. Geochim. Cosmochim. Acta 42, 1383–1389.
Rudkiewicz, J., Penteado, H.d.B., Vear, A., Vandenbroucke, M., Brigaud, F., Wendebourg, J., Duppenbecker, S., 2000. Integrated basin modeling helps to decipher petroleum systems. In: In: Mello, M., Katz, B. (Eds.), Petroleum Systems of South Atlantic Margins, Illustrated, vol. 2000. AAPG and PETROBRAS, pp. 27–40.
Rutter, E., Elliott, D., 1976. The kinetics of rock deformation by pressure solution. Phil. Trans. Roy. Soc. Lond.: Mathematical, Physical and Engineering Sciences 283, 203–219.
Saigal, G.C., Bjorlykke, K., Larter, S., 1992. The effects of oil emplacement on diagenetic processes: examples from the Fulmar reservoir sandstones, Central North sea: geologic note (1). AAPG (Am. Assoc. Pet. Geol.) Bull. 76, 1024–1033.
Sathar, S., Worden, R.H., Faulkner, D.R., Smalley, P.C., 2012. The effect of oil saturation

on the mechanism of compaction in granular materials: higher oil saturations lead to more grain fracturing and less pressure solution. J. Sediment. Res. 82, 571–584.
Sheldon, H.A., Wheeler, J., Worden, R.H., Cheadle, M.J., 2003. An analysis of the roles of stress, temperature, and pH in chemical compaction of sandstones. J. Sediment. Res. 73, 64–71.
Shimizu, I., 1995. Kinetics of pressure solution creep in quartz: theoretical considerations. Tectonophysics 245, 121–134.
Sibley, D.F., Blatt, H., 1976. Intergranular pressure solution and cementation of the Tuscarora orthoquartzite. J. Sediment. Res. 46, 881–896.
Stewart, D., 1986. Diagenesis of the shallow marine Fulmar Formation in the Central North sea. Clay Miner. 21, 537–564.
Storvoll, V., Bjørlykke, K., Karlsen, D., Saigal, G., 2002. Porosity preservation in reservoir sandstones due to grain-coating illite: a study of the Jurassic Garn Formation from the Kristin and Lavrans fields, offshore Mid-Norway. Mar. Petrol. Geol. 19, 767–781.
Stricker, S., Jones, S.J., Grant, N.T., 2016b. Importance of vertical effective stress for reservoir quality in the Skagerrak formation, central Graben, North Sea. Mar. Petrol. Geol. 78, 895–909.
Stricker, S., Jones, S.J., Sathar, S., Bowen, L., Oxtoby, N., 2016a. Exceptional reservoir quality in HPHT reservoir settings: examples from the Skagerrak formation of the Heron cluster, North Sea, UK. Mar. Petrol. Geol. 77, 198–215.
Swarbrick, R., Osborne, M., Grunberger, D., Yardley, G., Macleod, G., Aplin, A., Larter, S., Knight, I., Auld, H., 2000. Integrated study of the Judy field (block 30/7a)—an overpressured Central North sea oil/gas field. Mar. Petrol. Geol. 17, 993–1010.
Tada, R., Maliva, R., Siever, R., 1987. A new mechanism for pressure solution in porous quartzose sandstone. Geochim. Cosmochim. Acta 51, 2295–2301.
Tada, R., Siever, R., 1989. Pressure solution during diagenesis. Annu. Rev. Earth Planet Sci. 17, 89–118.
Taylor, A., Gawthorpe, R., 1993. Application of Sequence Stratigraphy and Trace Fossil Analysis to Reservoir Description: Examples from the Jurassic of the North Sea, Geological Society, London, Petroleum Geology Conference Series. Geological Society of London, pp. 317–335.
Taylor, T.R., Giles, M.R., Hathon, L.A., Diggs, T.N., Braunsdorf, N.R., Birbiglia, G.V., Kittridge, M.G., Macaulay, C.I., Espejo, I.S., 2010. Sandstone diagenesis and reservoir quality prediction: models, myths, and reality. AAPG (Am. Assoc. Pet. Geol.) Bull. 94, 1093–1132.
Taylor, T.R., Kittridge, M.G., Winefield, P., Bryndzia, L.T., Bonnell, L.M., 2015. Reservoir quality and rock properties modeling–Triassic and Jurassic sandstones, greater Shearwater area, UK Central North Sea. Mar. Petrol. Geol. 65, 1–21.
Thomson, A., 1959. Pressure Solution and Porosity. Society of Economic Paleontologists and Mineralogists SP7, pp. 92–110.
Valley, J.W., Kita, N.T., 2009. In situ oxygen isotope geochemistry by ion microprobe. MAC short course: secondary ion mass spectrometry in the earth sciences 41, 19–63.
van Noort, R., Spiers, C.J., Pennock, G.M., 2008. Compaction of granular quartz under hydrothermal conditions: controlling mechanisms and grain boundary processes. J. Geophys. Res.: Solid Earth 113, 1–23.
Walderhaug, O., 1994a. Temperatures of quartz cementation in Jurassic sandstones from the Norwegian continental shelf–evidence from fluid inclusions. J. Sediment. Res. 64, 311–323.
Walderhaug, O., 1994b. Precipitation rates for quartz cement in sandstones determined by fluid-inclusion microthermometry and temperature-history modeling. J. Sediment. Res. 64, 324–333.
Walderhaug, O., 1996. Kinetic modeling of quartz cementation and porosity loss in deeply buried sandstone reservoirs. AAPG (Am. Assoc. Pet. Geol.) Bull. 80, 731–745.
Walderhaug, O., 2000. Modeling quartz cementation and porosity in middle Jurassic brent group sandstones of the Kvitebjørn field, northern North Sea. AAPG (Am. Assoc. Pet. Geol.) Bull. 84, 1325–1339.
Warren, E., Smalley, P., Howarth, R., 1994. Compositional variations of North Sea formation waters. In: Warren, E., Smalley, P. (Eds.), North Sea Formation Waters Atlas. Geological Society London, pp. 119–140.
Weyl, P.K., 1959. Pressure solution and the force of crystallization: a phenomenological theory. J. Geophys. Res. 64, 2001–2025.
Wilkinson, M., Darby, D., Haszeldine, R.S., Couples, G.D., 1997. Secondary porosity generation during deep burial associated with overpressure leak-off: Fulmar Formation, United Kingdom Central Graben. AAPG (Am. Assoc. Pet. Geol.) Bull. 81, 803–813.
Wilkinson, M., Haszeldine, R.S., 1996. Aluminium loss during sandstone diagenesis. J. Geol. Soc. 153, 657–660.
Wilkinson, M., Haszeldine, R.S., 2011. Oil charge preserves exceptional porosity in deeply buried, overpressured, sandstones: central North Sea, UK. J. Geol. Soc. 168, 1285–1295.
Worden, R., Armitage, P., Butcher, A., Churchill, J., Csoma, A., Hollis, C., Lander, R., Omma, J., 2018a. Petroleum reservoir quality prediction: overview and contrasting approaches from sandstone and carbonate communities. Geol. Soc., London, Special Publications 435 SP435. 421.
Worden, R., Morad, S., 2000. Quartz Cementation in Oil Field Sandstones: a Review of the Key Controversies. Quartz Cementation in Sandstones, vol. 29. Special publications of international association of sedimentologists, pp. 1–20.
Worden, R.H., Bukar, M., Shell, P., 2018b. The effect of oil emplacement on quartz cementation in a deeply buried sandstone reservoir. AAPG (Am. Assoc. Pet. Geol.) Bull. 102, 49–75.
Worden, R.H., French, M.W., Mariani, E., 2012. Amorphous silica nanofilms result in growth of misoriented microcrystalline quartz cement maintaining porosity in deeply buried sandstones. Geology 40, 179–182.
Worden, R.H., Oxtoby, N.H., Smalley, P.C., 1998. Can oil emplacement prevent quartz cementation in sandstones? Petrol. Geosci. 4, 129–137.
Yardley, G., Swarbrick, R., 2000. Lateral transfer: a source of additional overpressure? Mar. Petrol. Geol. 17, 523–537.